Canadian Mineralogist
Vol. 30, pp. 319-326 (1992)

CHARACTERIZATION OF V–Sb–W-BEARING RUTILE FROM THE HEMLO GOLD DEPOSIT, ONTARIO

ANDREW J. URBAN, BERNARD F. HOSKINS* AND IAN E. GREY
CSIRO Division of Mineral Products, P.O. Box 124, Port Melbourne, Victoria 3207, Australia

ABSTRACT

V–Sb–W-bearing rutile, sampled in drill cores from the Hemlo gold deposit, Ontario, was studied by single-crystal X-ray diffraction and wavelength-dispersion electron-microprobe techniques. The grains studied contain up to 8 wt.% Sb_2O_5, 6% V_2O_3 and 5.9% WO_3. Single-crystal X-ray-intensity data were collected for Sb-rich [7.0 wt.% Sb_2O_5, *a* 4.5967(6), *c* 2.9657(3) Å] and W-rich grains [5.9 wt.% WO_3, *a* 4.5985(7), *c* 2.9616(7) Å]. The structures refined to an *R* of 1.50 and 1.72%, respectively, using 247 unique reflections with $\sin\theta/\lambda < 1.15$ Å^{-1}. The refinements show that the minor elements all substitute for titanium at the metal atom site. Interelement correlations in the microprobe results are consistent with three types of substitution: $2V^{3+} + W^{6+} \leftrightarrow 3Ti^{4+}$, $V^{3+} + Sb^{5+} \leftrightarrow 2Ti^{4+}$, and $V^{4+} \leftrightarrow Ti^{4+}$.

Keywords: V–Sb–W-bearing rutile, crystal structure, substituted rutile, Hemlo, Ontario.

SOMMAIRE

Une variété de rutile contenant V, Sb et W, prélevé dans des carottes du gisement d'or de Hemlo, en Ontario, a fait l'objet d'études par diffraction X sur cristaux uniques et par analyse à la microsonde électronique en dispersion d'énergie. Les grains contiennent jusqu'à 8% en poids de Sb_2O_5, 6% de V_2O_3 et 5.9% de WO_3. Les intensités de diffraction X ont été mesurées sur cristaux uniques d'une variété riche en Sb [7.0% Sb_2O_5, *a* 4.5967(6), *c* 2.9657(3) Å] et d'une autre riche en W [5.9% WO_3, *a* 4,5985(7), *c* 2.9616(7) Å]. Leur structure a été affinée à un résidu *R* de 1.50 et 1.72%, respectivement, avec 247 réflexions uniques ayant $\sin\theta/\lambda < 1.15$ Å^{-1}. Les résultats des affinements montrent que les éléments mineurs remplacent le titane sur le site de l'atome métallique. Les corrélations inter-éléments dans les résultats analytiques concordent avec trois schémas de substitution: $2V^{3+} + W^{6+} \leftrightarrow 3Ti^{4+}$, $V^{3+} + Sb^{5+} \leftrightarrow 2Ti^{4+}$, et $V^{4+} \leftrightarrow Ti^{4+}$

(Traduit par la Rédaction)

Mots-clés: rutile vanadifère, antimonifère et tungstenifère, structure cristalline, rutile substitué, Hemlo, Ontario.

INTRODUCTION

The rich gold deposits at Kalgoorlie, Western Australia, and Hemlo, Ontario, have in common a close relationship between gold and vanadium. The main vanadium-bearing mineral in both deposits is a vanadian muscovite containing up to 12 wt.% V_2O_3 (Nickel 1977, Harris 1989). It shows a strong spatial association with gold mineralization; patches and bands of the bright green mineral are well recognized by miners as being associated with particularly high gold values. Other vanadium-bearing minerals common to the two deposits are tomichite, $(V,Fe)_4Ti_3AsO_{13}(OH)$, which contains Ba at Hemlo, and vanadian hematite (Grey *et al.* 1987, Nickel & Grey 1986), both containing up to ~40 wt. % V_2O_3. At Kalgoorlie, vanadium is found as a major element in the oxide minerals nolanite, tivanite and vanadian magnetite – coulsonite (Nickel & Grey 1986), whereas at Hemlo, vanadium also occurs in vanadian grossular, titanite, hemloite, rutile, pumpellyite, epidote and vesuvianite (Harris 1989, Pan & Fleet 1992). Hemloite, ideally $(As,Sb)_2(Ti,V,Fe,Al)_{12}O_{23}OH$, is a new mineral that is compositionally and structurally related to tomichite (Harris *et al.* 1989). Vanadium-bearing rutile containing up to ~6 wt. % V_2O_3 is the principal oxide mineral in the Hemlo deposit, and it appears to define the ore zone (Harris 1989). The rutile is unusual in containing considerable amounts of antimony and tungsten, up to 8 wt.% Sb_2O_5 and 5.9 wt.% WO_3, respectively. There seems to be no previously reported studies on naturally occurring V–Sb–W-bearing rutile. We were interested in determining the oxidation states of the minor

---

*Department of Chemistry, University of Melbourne, Parkville, Victoria 3052, Australia.

elements and in establishing the way in which they were incorporated into the rutile structure, through substitution or in interstitial sites. We report here the results of single-crystal X-ray structure refinements and electron-microprobe analyses on V–Sb–W-bearing rutile crystals from two mines within the Hemlo deposit.

PREVIOUS STUDIES ON V, Sb AND W IN RUTILE-TYPE STRUCTURES

The literature on incorporation of V, Sb and W into rutile-type TiO_2 is sparse and is restricted to reports of studies on synthetic materials. Both VO_2 and WO_2 crystallize with monoclinic distortions of the tetragonal rutile structure due to metal–metal bonding. They form extensive solid-solutions with TiO_2 at elevated temperatures (Chang *et al.* 1967, Sakata & Sakata 1967). Electron-spin resonance studies on V-doped TiO_2 confirm that V^{4+} substitutes for Ti^{4+} in the tetragonal rutile structure (Gerritsen & Lewis 1960).

There is some controversy in the literature regarding antimony-doped TiO_2. Krause (1968) noted that incorporation of antimony into TiO_2 is very limited when the reaction is conducted in nitrogen, but is more extensive for reaction in air. He proposed that charge balance was maintained in the rutile structure by a mixture of Sb^{3+} and Sb^{5+}. In a more recent study, Morita *et al.* (1987) carried out studies of electron spectroscopy to measure the binding energy of antimony in doped rutile. Their results were interpreted in terms of substitution of Sb^{3+} for Ti^{4+}, together with creation of oxygen vacancies. Berry and coworkers have studied antimony doping in rutile-type TiO_2 and SnO_2. For doped TiO_2, ^{121}Sb Mössbauer spectra (Berry & Gogarty 1988) show a single absorption peak, which was ascribed to Sb^{5+}, whereas for doped SnO_2, the results of a neutron-diffraction study were interpreted as incorporation of interstitial Sb^{3+} even though the Mössbauer spectrum was found to be consistent with predominantly Sb^{5+} (Berry & Greaves 1981). The problems encountered in establishing the oxidation state of the antimony may arise from charge transfer between Sb^{3+} and Sb^{5+} (Pyke *et al.* 1978).

Mixed-metal dioxides with rutile-related structures have been extensively studied for combinations of V, Sb and W with each other and with other elements (Bayer 1962, Donaldson *et al.* 1975). The phase systems studied are complex and contain variable valence states. For example, the pseudobinary system VO_2–WO_2 contains five different solid-solution phases that are all structurally closely related to rutile (Israelsson & Kihlborg 1970). Although both end-member compositions contain M^{4+}, the composition $W_{0.33}V_{0.67}O_2$ was shown from a single-crystal X-ray refinement to contain W^{6+} and V^{3+} (Hodeau *et al.* 1978). By analogy with $W_{0.33}V_{0.67}O_2$, the composition $W_{0.5}V_{0.5}O_2$ was proposed to contain W^{4+}, W^{6+} and V^{3+} (Nii *et al.* 1979). However, in the monoclinic rutile-like structure of $Al_{0.5}W_{0.5}O_2$, the tungsten was confirmed to be present as W^{5+}, stabilized by W–W bonds (Doumerc *et al.* 1975).

The mixed dioxide of antimony and vanadium has received considerable attention. Although originally interpreted to contain Sb^{3+} and V^{5+} (Vernon & Milligan 1951), studies by Mössbauer spectroscopy showed that the oxidation states are Sb^{5+} and V^{3+} (Birchall & Sleight 1976). Stoichiometric $V_{0.5}Sb_{0.5}O_2$ could not be prepared. Different nonstoichiometric phases form, depending on the composition of the reaction atmosphere (Berry *et al.* 1983, Birchall & Sleight 1976). An ESR study by Sunandana (1984) confirmed the existence of an antimony-deficient MO_2 tetragonal rutile phase containing V^{4+}, *i.e.*, $V^{3+}_{1-x}V^{4+}_{2x}Sb^{5+}_{1-x}O_4$, $X \approx 0.1$. Antimony has been shown by Mössbauer spectroscopy to be pentavalent in a number of rutile-type $M_{0.5}Sb_{0.5}O_2$ and trirutile-type $M_{0.33}Sb_{0.67}O_2$ antimonates (Wooten *et al.* 1974).

In mixed-metal dioxides, the formation of the rutile structure is favored for oxidation states of the metal atoms that give similar *M*–O distances and small distortions (Bernier & Poix 1967, Hodeau *et al.* 1978). On this basis, and on the evidence given above, the most probable oxidation states for V, Sb and W in doped rutile are V^{3+} and V^{4+}, Sb^{5+}, W^{5+} and W^{6+}.

OCCURRENCE AND SAMPLE DESCRIPTIONS

The Hemlo gold deposit is located near Marathon on the northeastern shore of Lake Superior, in a sequence of Archean metasedimentary and volcanic rocks that form the Hemlo – Heron Bay greenstone belt. The deposit is unique in terms of the intense tectonic deformation of the rock sequences and the complex suite of minerals. The ore zone contains at least 80 million tonnes of gold at 7.7 g/t Au and is enriched in Mo, Sb, As, Hg, Tl, V and Ba. Details of the mineralogy and geochemistry of the deposit and references to regional and local geology are reported by Harris (1989).

The ore zone is characterized in part by the variable presence of molybdenite, green vanadian muscovite and V–Sb–W-bearing rutile. Samples of the latter mineral have been studied by Harris (1989) in polished sections of material taken from drill core from each of the three currently mined properties, *i.e.*, the David Bell, Golden Giant and Williams mines. Polished sections of material taken from drill holes TC218W from the David Bell mine at 767.5 m, and W70 from the Williams mine at 761.4 m, were kindly provided for our studies by D.C. Harris, Geological Survey of Canada. The rutile in these two samples contains some of the highest levels of W and Sb recorded (Harris 1989).

Drill core TC218W contains particularly high concentrations of gold, up to 100 g/t for some 1-m intersections. The main ore-zone is intersected by the drill hole from 763.8 to 775.1 m (Harris 1989). The ore minerals are stibnite, native gold and mercury-bearing sphalerite. They are associated with abundant molybdenite, vanadian muscovite, barian microcline, barite and V–Sb–W-bearing rutile. In the polished section taken from core at 767.5 m, the rutile grains occur in a matrix of barian microcline. Closely associated minerals are quartz, pyrite and molybdenite. The rutile grains are anhedral and irregular in shape and vary in size from 250 × 100 μm to 30 × 30 μm. When extracted from the polished section they are in the form of dark brown, stubby anhedral to subhedral crystals.

Drill hole W70 is located close to the boundary between the Williams and Golden Giant mines, virtually in the center of the deposit, where the ore zone is 45 m thick (Harris 1989). In the drill core, the gold zone extends from 709 to 781 m. At ~760 m, from where the polished section was taken, the main minerals are pyrite, molybdenite, stibnite, realgar, barite, barian microcline, vanadian muscovite and V–Sb–W-bearing rutile. The rutile in this section is Sb-rich and W-poor, with Sb_2O_5 and WO_3 contents of typically 5-8 and 0.5-1 wt.%, respectively. The rutile grains are anhedral and occasionally contain quartz inclusions. They are commonly rimmed with titanite, as has been previously observed for hemloite–rutile associations (Fig. 1 in Harris *et al.* 1989). The grains range in size from 150 × 100 μm to 50 × 25 μm. They generally occur in a barite or quartz – K-feldspar matrix and are locally penetrated by molybdenite needles, as illustrated in Figure 1.

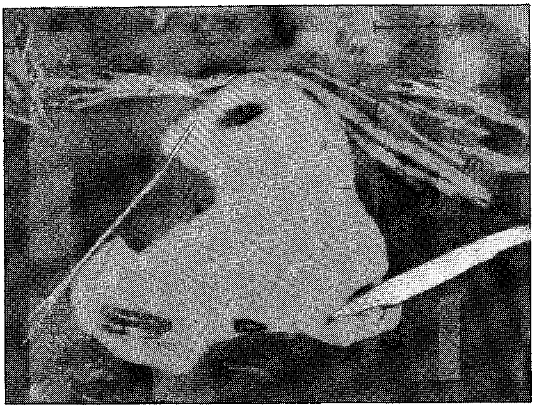

FIG. 1. Optical photomicrograph of Sb-rich rutile in a matrix of barian microcline. The grain contains quartz inclusions (black) and is penetrated by needles of molybdenite (white). The scale bar represents 100 μm.

EXPERIMENTAL

Wavelength-dispersion (WD) analyses were made using a Cameca Camebax electron microprobe. The accelerating voltage used was 20 kV, and the beam current, 15 nA. Counting time on peaks and backgrounds was 20 s. Matrix corrections are those of Pouchou & Pichoir (1984). The following standards were used: $CaWO_4$ (W$L\alpha$), Sb_2S_3 (Sb$L\alpha$), Fe_2O_3 (Fe$K\alpha$), TiO_2 (Ti$K\alpha$) and V metal (V$K\alpha$). Antimony was analyzed for

TABLE 1. CRYSTAL DATA AND DETAILS OF STRUCTURE DETERMINATION OF Sb-V-W-BEARING RUTILE

Crystal	W-rich rutile	Sb-rich rutile
TiO_2 wt. %	84.90	89.05
V_2O_3	6.09	3.95
FeO	0.19	0.10
Sb_2O_5	2.63	7.02
WO_3	5.87	1.33
Total	99.68	101.45
Formula	$V_{0.069}Sb_{0.014}W_{0.022}Ti_{0.894}O_2$	$V_{0.041}Sb_{0.033}W_{0.005}Ti_{0.917}O_2$
Fw	84.00	83.08
Crystal System	Tetragonal	Tetragonal
Space Group	$P4_2/mnm$	$P4_2/mnm$
a, Å	4.5985(7)	4.5967(6)
c, Å	2.9616(7)	2.9657(3)
Vol., $Å^3$	62.63	62.66
Z	2	2
ρ (cal), g cm^{-3}	4.45	4.40
Crystal dimensions (mm)	Tabular (0.065 x 0.095 x 0.111)	Approx. Spherical (radius = 0.075)
F(000)	79.06	78.46
μ, cm^{-1}	81.99	70.26
min., max. trans. factors	0.2162; 0.3948	0.4292; 0.4816
Scan Technique	$\omega : 2\theta$	$\omega : 2\theta$
Scan Angle ω (°), atanθ + b	a 0.75; b 0.35	a 0.75; b 0.35
Fixed Diameter Aperture, mm	2.40	2.40
2θ range (°)	$2 \leq 2\theta \leq 110$	$2 \leq 2\theta \leq 110$
hkl range	$-10 \leq h \leq 10$ $-10 \leq k \leq 10$ $-6 \leq l \leq 6$	$-10 \leq h \leq 10$ $-10 \leq k \leq 10$ $-6 \leq l \leq 6$
No. of Meas. Reflect.	3232	3238
No. of Unique Reflect.	247	248
R_{amal}	0.0365	0.0129
No. of Variables	11	11
Refinement	full-matrix least-squares; function minimized $\Sigma w\Delta^2$	
Weighting Scheme:		
$w = [k/(\sigma_F^2 + g\|F\|^2)]$	k = 10.67 g = 0.0001 fixed	k = 6.49 g = 0.0001 fixed
Isotropic Extinction Parameter	2.21(10) x 10^{-5}	2.56(8) x 10^{-5}
Final R ($\Sigma\|\Delta F\|/\Sigma\|F_o\|$)	0.0172	0.0150
Final wR ($\Sigma w^{1/2}\|\Delta F\|/\Sigma w^{1/2}\|F_o\|$)	0.0177	0.0149
Max. shift/esd	-0.008	0.018
Max. residual electron density, e $Å^{-3}$	0.50	0.47

using a PET crystal, and the other elements were sought using a LiF crystal. Special care was taken in selecting the background positions for the V*K*α peak to minimize interference from the adjacent Ti*K*β peak. Analyses on the pure titania standard showed that the vanadium would be underestimated by no more than 2.4% relative. Quantitative energy-dispersion (ED) analyses were used to characterize high-Sb and high-W grains used in the crystal-structure refinements. The ED analyses were obtained on a JEOL JSM 25S scanning electron microscope fitted with a LINK 860 Series 2 ED system. Samples were analyzed at 15 kV and 0.8 nA, using a counting time of 50 s. Standards were as for the electron-microprobe analyses, with the exception of tungsten (W metal, W*M*α).

Intensity data were collected on single crystals using an Enraf–Nonius CAD4F diffractometer equipped with a graphite monochromator and employing Mo*K*α radiation (λ = 0.71069 Å). Accurate values of the unit-cell parameters were determined from least-squares refinement of the angular settings of 25 centered reflections with $11 < \theta < 18°$. Details of the data collection are given in Table 1. Intensity measurements were made with the $\omega - 2\theta$ mode. Three strong reflections were used as orientation controls (every 100 reflections) and as intensity monitors (every 9600 s). A full sphere of data to $\theta = 55°$ was collected for each of two crystals. Corrections for Lorentz, polarization and absorption were applied. The absorption correction was numerical, based on indexing of the faces of the crystals (Sheldrick 1976). Structure refinements were performed using the SHELX-76 system (Sheldrick 1976). Scattering curves for neutral atoms, together with corrections for anomalous dispersion, were taken from the International Tables for X-ray Crystallography (1974).

SINGLE-CRYSTAL X-RAY STUDIES

Crystals having high contents of Sb and W from ED analyses were removed from the polished sections and checked using the precession method. The first crystal examined was found to be twinned on (101) (rutile elbow twin). Subsequently, single-crystal examples of high-W and high-Sb grains were obtained, and sets of intensity data were collected as described in the Experimental section and Table 1. The same procedure of refinement was followed for both crystals and is described below for the high-Sb crystal. The refinement was initiated using published structural data for rutile (Gonschorek 1982) and with titanium only in the metal atom site. The occupancy of the titanium site was established from the ED analyses. Refinement of coordinates and isotropic thermal parameters gave an *R* value of 0.04. A difference Fourier map was calculated to check if the minor elements occupy interstitial sites or substitute at the titanium site. No evidence was found for occupancy of interstitial sites; the only significant electron density occurs at the titanium site. Refinement of the occupancy factor, SOF, of the titanium site, atomic coordinates, anisotropic thermal parameters and an empirical extinction parameter (Sheldrick 1976) led to convergence at $R = 0.015$, $wR = 0.015$ for all 248 reflections. The weighting scheme used was of the form $w = k/(\sigma^2 + 0.0001F^2)$. The titanium SOF refined to 0.1302(2), giving a site occupancy of 1.042. The value is higher than 1 because of substitution of higher-atomic-number elements for titanium. The final refinement was repeated with the minor elements V, W and Sb included with titanium at the metal atom site. Their SOF values were fixed at the numbers obtained from the ED analyses, and their anisotropic thermal parameters were constrained to be equal to those of titanium. The *R* and *wR* values remained unchanged, and the parameters were not significantly different from the refinement with only titanium at the metal atom site. Details of the refinement for Sb-rich and W-rich crystals are given in Table 1. Refined coordinates, anisotropic thermal parameters and values of SOF are given in Table 2. The observed and calculated structure-factors have been submitted to the Depository of Unpublished Data, CISTI, National Research Council of Canada, Ottawa, Canada K1A 0S2.

ELECTRON-MICROPROBE DATA

Following the preliminary survey of rutile grains using ED analyses to select crystals for structure

TABLE 2. FRACTIONAL ATOMIC COORDINATES, ANISOTROPIC THERMAL PARAMETERS* AND SITE OCCUPATION FACTORS (SOF)

	W-rich	**Sb-rich**	**Pure Rutile**†
Metal (0,0,0)			
Refined SOF for Titanium at metal site.	0.1328(9)	0.1302(7)	0.125
$U_{11}(=U_{22})$	0.00784(7)	0.00698(6)	0.00668(4)
U_{33}	0.00633(9)	0.00587(8)	0.00481(7)
U_{12}	0.00008(3)	-0.00008(2)	-0.00012(3)
Oxygen (x,x,0)			
x	0.30469(7)	0.30474(6)	0.30491(5)
$U_{11}(=U_{22})$	0.00643(11)	0.00604(10)	0.00531(6)
U_{33}	0.00581(14)	0.00504(12)	0.0040(1)
U_{12}	-0.00205(12)	-0.00196(10)	-0.0018(1)

* The temperature term has the form $\exp\left(-2\pi^2 \sum_{i=1}^{3} \sum_{j=1}^{3} U_{ij} h_i h_j a_i^* a_j^*\right)$

† For comparison, the parameters for pure rutile (Gonschorek 1982) are given in the last column.

TABLE 3. CHEMICAL COMPOSITION (WD ELECTRON-MICROPROBE DATA) OF SB-V-W-(FE)-BEARING RUTILE

(a) Polished block HEMLO TECK H218W 767.5m.

	1	2	3	4	5	6	7	8	9	10	11	12
WO_3	5.24	3.01	1.57	4.91	4.25	1.50	5.27	5.00	1.94	5.16	1.48	5.62
V_2O_3	4.47	3.38	2.51	3.92	3.64	2.65	4.18	5.10	3.09	5.42	2.70	4.86
TiO_2	86.66	87.87	89.70	85.41	85.24	91.41	85.43	85.60	91.02	85.27	89.81	86.11
Sb_2O_5	2.85	2.83	3.29	2.76	3.03	3.23	2.66	2.81	3.45	3.05	3.60	2.83
FeO	0.56	0.51	0.36	0.71	0.63	0.34	0.77	0.22	0.33	0.21	0.27	0.48
Total	99.77	97.60	97.42	97.71	96.78	99.12	98.30	98.74	99.83	99.11	97.85	99.89

(b) Polished block LAC W70 761.4m.

	1	2	3	4	5	6	7	8	9	10	11	12
WO_3	0.72	0.49	1.10	0.45	0.51	0.79	0.89	0.61	0.20	0.91	0.67	0.32
V_2O_3	2.86	3.61	4.24	4.03	3.26	3.99	3.22	3.98	2.30	3.06	2.58	4.14
TiO_2	89.43	88.62	87.19	88.35	90.30	87.50	90.17	86.24	92.72	88.44	88.98	85.89
Sb_2O_5	5.03	7.30	7.65	7.43	5.92	5.05	5.33	7.92	4.31	4.77	4.36	6.73
FeO	0.02	0.02	0.05	0.05	0.02	0.00	0.02	0.08	0.04	0.04	0.00	0.00
Total	98.05	100.04	100.23	100.31	100.00	97.34	99.63	98.82	99.57	97.22	96.59	97.08

Concentrations are reported in wt.%.

refinements, a systematic electron-microprobe analysis of all rutile grains in the two sections supplied was undertaken using WD. A selection of these results is presented in Table 3. The full set of data has been deposited (see previous section).

The presentation of the results as oxides TiO_2, WO_3, V_2O_3, Sb_2O_5 and Fe_2O_3 is consistent with determinations of valence states from the microprobe results (see Discussion). In sample W70, the Sb_2O_5 content of the rutile is high, averaging 5.9 wt.%. Harris (1989) has noted that the W70 drill hole contains a number of antimony-rich ore minerals, including stibnite, tetrahedrite, zinkenite and aurostibite. The V_2O_3 content averages 3.5 wt.%, whereas the average WO_3 content is only 0.7 wt.%. In contrast, the TC218W sample has a relatively high average WO_3 content, 3.9 wt.%, with individual values ranging from 1.5 to 5.3 wt.%. The average Sb_2O_5 content, 3.0 wt.%, is lower than in the W70 sample. The Sb_2O_5 content varies over a relatively narrow range, 2.7 to 3.6 wt.%. Both Sb in W70 and W in TC218W show strong positive correlations with V, as discussed below.

DISCUSSION

The single-crystal refinements of the structure of V–Sb–W-bearing rutile confirm that the minor elements all substitute for titanium in the rutile structure. As seen from Table 2, the refined parameters for the W-rich and Sb-rich rutiles are very similar to those for synthetic TiO_2; the major difference lies in the U_{33} parameter, which is 20–30% higher for the natural rutile. The thermal parameters are consistently higher for the W-rich rutile. This is at least in part due to inadequate modeling of absorption for the less regularly shaped W-rich crystal; compare the R_{amal} values in Table 1. The increase in the mean-square displacements for M and O is only of the order of 0.005 Å, indicating that the metals substituting for titanium have closely matching sizes. This is consistent with the conclusion drawn in the Previous Studies section that the most likely oxidation states are Sb^{5+}, W^{5+} or W^{6+} and V^{3+} or V^{4+}

Information on charge-coupled substitutions for Ti^{4+} (*e.g.*, $V^{3+} + W^{5+} \leftrightarrow 2Ti^{4+}$) and hence oxidation states, can be obtained from the electron-microprobe data by plotting $[M_1]$ *versus* $[M_2]$ atom fractions. These are illustrated in Figures 2a and b for the W-rich and Sb-rich rutile, respectively. It is clear that the [V] *versus* [W] data for W-rich rutile lie along a line of slope 2, corresponding to a coupled substitution of the type $2V^{3+} + W^{6+} \leftrightarrow 3Ti^{4+}$. The [V] *versus* [Sb] data for Sb-rich rutile show greater scatter, and they lie more closely along a line of slope 1, corresponding to the coupled substitution $V^{3+} + Sb^{5+} \leftrightarrow 2Ti^{4+}$.

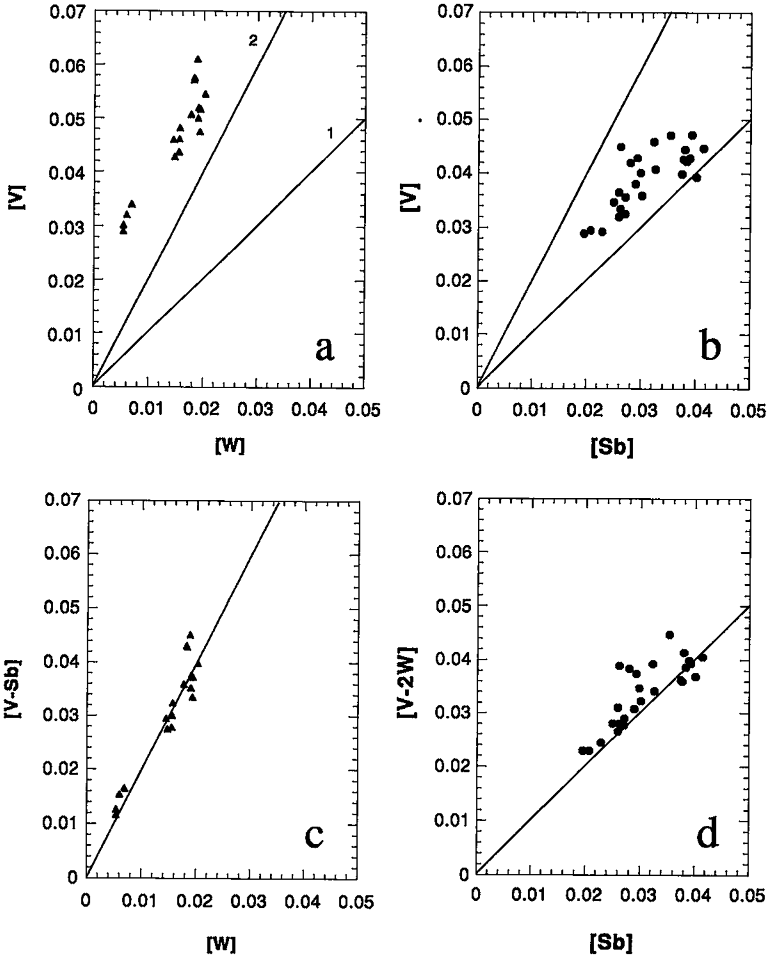

FIG. 2. Element-element plots (atom fractions) of electron-microprobe data for W-rich rutile (a and c), and for Sb-rich rutile (b and d). The atom fractions have been normalized to $\Sigma[M] = 1$.

In both cases, the lines have to be translated parallel to the [V] axis to give a good fit to the data points. The intercept on the [V] axis corresponds to the amount of V needed to compensate for the average content of the other minor element (Sb in W-rich rutile and *vice versa*). In Figures 2c and d, this has been taken into account by plotting [V–Sb] *versus* [W] and [V–2W] *versus* [Sb]. The corrected data for the W-rich crystals are modeled satisfactorily by a line of slope 2 passing through the origin. A regression analysis gives the equation $[V-Sb] = 0.002(3) + 1.89(16)[W]$ ($R = 0.95$). For the Sb-rich rutile, the data points lie consistently to the high-[V–2W] side of the line of slope 1 through the origin. This may be explained by a variable amount of V^{4+}, as proposed for nonstoichiometric $VSbO_4$ (Birchall & Sleight 1976). The very low levels of iron in the rutile were not considered, but by analogy with other reported examples of iron-bearing rutile (Putnis 1978), the iron is expected to be trivalent.

The V–Sb–W-bearing rutile is a solid solution involving the end members WV_2O_6, $VSbO_4$ and TiO_2, together with minor VO_2 in the Sb-rich samples. Using published unit-cell parameters for TiO_2 (Abrahams & Bernstein 1971), WV_2O_6 (Hodeau *et al.* 1978) and $VSbO_4$ (Berry *et al.* 1983), the parameters were calculated for the two crystals used in the structure refinements. Notwithstanding the possibility of errors due to nonlinear mixing (Newton & Wood 1980), the calculated values agree with the refined values given in Table 1 to within

0.001 Å, confirming the observed anisotropic change in the cell dimensions (*a* decreases whereas *c* increases from the W-rich to the Sb-rich crystal). The general formula for V-Sb-W-bearing rutile can be written as $W^{6+}{}_{0.333x}Sb^{5+}{}_{0.5y}(V^{3+},Fe^{3+})_{0.667x+0.5y}(Ti^{4+},V^{4+})_{1-x-y}O_2$.

It is interesting to note that rutile and hemloite, which are both Sb-containing titanates found in close proximity in the Hemlo deposit, have antimony in the pentavalent and trivalent oxidation states, respectively. Evidently, the different oxidation states of the same element occurring in coexisting oxides reflect the different site-stabilization energies in the two structures.

ACKNOWLEDGEMENTS

We are indebted to D.C. Harris for supplying the drill-core samples and for providing information on the mineralogy and geochemistry of the Hemlo gold deposit. We thank I. Harrowfield, P. Rummel and C. MacRae for help with the electron microprobe and ED analyses. We appreciate the care and thoroughness taken by M.E. Fleet and an anonymous reviewer, whose comments significantly improved the original manuscript.

REFERENCES

ABRAHAMS, S.C. & BERNSTEIN, J.L. (1971): Rutile: normal probability plot analysis and accurate measurement of crystal structure. *J. Chem. Phys.* **55**, 3206-3211.

BAYER, G. (1962): Isomorphie- und Morphotropiebeziehungen bei Oxyden mit TiO_2-Typ und verwandten Strukturen. *Ber. Dtsch. Keram. Ges.* **11**, 535-554.

BERNIER, J.C. & POIX, P. (1967): Etude cristallographique et magnétique d'un oxyde trirutile antiferromagnétique. *C.R. Acad. Sci. Paris* **265C**, 1247-1249.

BERRY, F.J., BRETT, M.E. & PATTERSON, W.R. (1983): Structural investigations of the vanadium - antimony - oxygen system. *J. Chem. Soc., Dalton Trans.*, 13-17.

______ & GOGARTY, P.M. (1988): Antimony-doped rutile titanium (IV) oxide. *J. Chem. Soc., Dalton Trans.*, 2167-2170.

______ & GREAVES, C. (1981): A neutron diffraction investigation of the defect rutile structure of tin-antimony oxide. *J. Chem. Soc., Dalton Trans.*, 2447-2451.

BIRCHALL, T. & SLEIGHT, A.W. (1976): Oxidation states in "$VSbO_4$". *Inorg. Chem.* **15**, 868-870.

CHANG, L.L.W., SCROGER, M.G. & PHILLIPS, B. (1967): High-temperature, condensed-phase equilibriums in the system Ti-W-O. *J. Less-Common Metals* **12**, 51-56.

DONALDSON, J.D., KJEKSHUS, A., NICHOLSON, D.G. & RAKKE, T. (1975): Properties of Sb-compounds with rutile-like structures. *Acta Chem. Scand.* **A 29**, 803-809.

DOUMERC, J.P., VLASSE, M., POUCHARD, M. & HAGENMULLER, P. (1975): Synthèse, croissance cristalline, propriétés structurales et physiques d'un nouveau tungstate +V d'aluminium $AlWO_4$. *J. Solid State Chem.* **14**, 144-151.

GERRITSEN, H.J. & LEWIS, H.R. (1960): Paramagnetic resonance of V^{4+} in TiO_2. *Phys. Rev.* **119**, 1010-1012.

GONSCHOREK, W. (1982): X-ray charge density study of rutile (TiO_2). *Z. Kristallogr.* **160**, 187-203.

GREY, I.E., MADSEN, I.C. & HARRIS, D.C. (1987): Barian tomichite, $Ba_{0.5}(As_2)_{0.5}Ti_2(V,Fe)_5O_{13}(OH)$, its crystal structure and relationship to derbylite and tomichite. *Am. Mineral.* **72**, 201-208.

HARRIS, D.C. (1989): The mineralogy and geochemistry of the Hemlo gold deposit, Ontario. *Geol. Surv. Can., Econ. Geol. Rep.* **38**.

______, HOSKINS, B.F., GREY, I.E., CRIDDLE, A.J. & STANLEY, C.J. (1989): Hemloite $(As,Sb)_2(Ti,V,Fe,Al)_{12}O_{23}OH$: a new mineral from the Hemlo gold deposit, Hemlo, Ontario, and its crystal structure. *Can. Mineral.* **27**, 427-440.

HODEAU, J.L., GONDRAND, M., LABEAU, M. & JOUBERT, J.C. (1978): Structure cristalline de WV_2O_6 sur monocristal à 298 et 383 K. *Acta Crystallogr.* **B34**, 3543-3547.

INTERNATIONAL TABLES FOR X-RAY CRYSTALLOGRAPHY, VOL. IV (1974): Kynoch Press, Birmingham, England.

ISRAELSSON, M. & KIHLBORG, L. (1970): The phase relations in the VO_2-WO_2 system. *Mat. Res. Bull.* **5**, 19-29.

KRAUSE, H.B. (1968): Mixed rutile crystal formation in the titanium-nickel-antimony-oxygen system. II. Mechanism of rutile solid solution. *Mat. Res. Bull.* **3**, 241-251.

MORITA, N., ENDO, T., SATO, T. & SHIMADA, M. (1987): The oxidation state of antimony and electrical properties in antimony-doped rutile. *J. Solid State Chem.* **68**, 106-111.

NEWTON, R.C. & WOOD, B.J. (1980): Volume behavior of silicate solid solutions. *Am. Mineral.* **65**, 733-745.

NICKEL, E.H. (1977): Mineralogy of the "green leader" gold ore at Kalgoorlie, Western Australia. *Aust. Inst. Min. Metall. Proc.* **263**, 9-13.

______ & GREY, I.E. (1986): A vanadium-rich mineral assemblage associated with the gold telluride ore at Kalgoorlie, Western Australia. *Proc. 13th Meeting, Intern. Mineral. Assoc.* (*Varna, Bulgaria, 1982*), 899-908.

NII, J., WAKIHARA, M. & TANIGUCHI, M. (1979): Phase relations in the $V_xW_{1-x}O_2$ system ($0.2 < x < 0.75$). *Mat. Res. Bull.* **14**, 1069-1074.

PAN, YUANMING & FLEET, M.E. (1992): Mineral chemistry and geochemistry of vanadian silicates in the Hemlo gold deposit, Ontario, Canada. *Contrib. Mineral. Petrol.* **109**, 511-525.

POUCHOU, J.L. & PICHOIR, F. (1984): A new model for quantitative X-ray microanalysis. *Rech. Aérosp.* **3**, 167-192.

PUTNIS, A. (1978): The mechanism of exsolution of hematite from iron-bearing rutile. *Phys. Chem. Miner.* **3**, 183-197.

PYKE, D., REID, R. & TILLEY, R.J.D. (1978): An electron microscope study of tin dioxide and antimony-doped tin dioxide. *J. Solid State Chem.* **25**, 231-237.

SAKATA, K. & SAKATA, T. (1967): Preparation and structural data of $(Ti_xV_{1-x})O_2$. *Jap. J. Appl. Phys.* **6**, 112.

SHELDRICK, G.M. (1976): *SHELX-76: A Programme for Crystal Structure Determination.* Univ. Cambridge, Cambridge, England.

SUNANDANA, C.S. (1984): ESR evidence for the existence of rutile-type, nonstoichiometric vanadium antimonate. *Mat. Res. Bull.* **19**, 325-329.

VERNON, L.W. & MILLIGAN, W.O. (1951): Crystal structure of rutile-like heavy metal orthovanadates. *Tex. J. Sci.* **3**, 82-85.

WOOTEN, J.B., LONG, G.G. & BOWEN, L.H. (1974): An ^{121}Sb Mössbauer study of metal antimonates. *J. Inorg. Nucl. Chem.* **36**, 2177-2183.

Received May 15, 1991, revised manuscript accepted November 13, 1991.